

Influence of electromagnetic interferences on the gravimetric sensitivity of surface acoustic waveguides.

L. Francis^a, J.-M. Friedt^b, R. De Palma^b, P. Bertrand^a and
A. Campitelli^b

^a*PCPM, Université catholique de Louvain, 1 Place Croix du Sud, B-1348
Louvain-la-Neuve, Belgium*

^b*Biosensors Group, IMEC, 75 Kapeldreef, B-3001 Leuven, Belgium*

Abstract

Surface acoustic waveguides are increasing in interest for (bio)chemical detection. The surface mass modification leads to measurable changes in the propagation properties of the waveguide. Among a wide variety of waveguides, Love mode has been investigated because of its high gravimetric sensitivity. The acoustic signal launched and detected in the waveguide by electrical transducers is accompanied by an electromagnetic wave; the interaction of the two signals, easily enhanced by the open structure of the sensor, creates interference patterns in the transfer function of the sensor. The influence of these interferences on the gravimetric sensitivity is presented, whereby the structure of the entire sensor is modelled. We show that electromagnetic interferences generate an error in the experimental value of the sensitivity. This error is different for the open and the closed loop configurations of the sensor. The theoretical approach is completed by the experimentation of an actual Love mode sensor operated under liquid in open loop configuration. The

experiment indicates that the interaction depends on the frequency and the mass modifications.

Key words: surface acoustic waves, electromagnetic waves, Love mode, interferences, gravimetric sensitivity

1 Introduction

Acoustic waves guided by the surface of solid structures form waveguides used as delay lines and filters in telecommunications (1). Waveguides support different modes with specific strain and stress fields (2). The acoustic velocity of each mode depends on different intrinsic and extrinsic parameters such as the mechanical properties of the materials, the temperature or the applied pressure. Waveguides are used as sensors when the velocity change is linked to environmental changes. For gravimetric sensors, the outer surface of the waveguide is exposed to mass changes. Due to the confinement of the acoustic wave energy close to the surface, these sensors are well suited for (bio)chemical sensors operating in gas or liquid environments. Among a wide variety of waveguides used for that purpose, Love mode sensors have attracted an increasing interest during the last decade (3; 4; 5; 6). A Love mode is guided by a solid overlayer deposited on top of a substrate material. The usual substrates are piezoelectric materials like quartz, lithium tantalate and lithium niobate (7). Associated to specific crystal cut of these substrates, the Love mode presents a shear-horizontal polarization that makes it ideal for sensing in liquid media.

Email address: francis@pcpm.ucl.ac.be (L. Francis).

Current research in Love mode sensors concerns the guiding materials in order to obtain a high gravimetric sensitivity. Typical materials under investigations are dielectrics like silicon dioxide and polymers, and more recently semiconductors with piezoelectric properties like zinc oxide (8; 9; 10; 11). Although the dispersion relation for Love mode is well set and the dependence of the gravimetric sensitivity of the liquid loaded sensor to the overlayer thickness has been thoroughly investigated (12; 13; 14; 15), little has been devoted to study the role played by the structure of the sensor and the transducers.

In this paper, we investigate the role played by the structure of the sensor and the interferences between the acoustic and the electromagnetic waves on the gravimetric sensitivity. In the first part, we present a model of the transfer function including the influence of electromagnetic interferences. In the second part, we show how these interferences modify the gravimetric sensitivity in open and closed loop configurations of the sensor. Finally, these effects are illustrated experimentally on a Love mode sensor.

2 Modelling

Waveguide sensors consist of a transducing part and a sensing part. The transducing part includes the generation and the reception of acoustic signals and their interfacing to an electrical instrumentation. The most common transducers are the widespread interdigital transducers (IDTs) on piezoelectric substrates introduced by White and Voltmer in 1965 (16). Although the transducing part can be involved in the sensing part, practical sensing is confined to the spacing between the transducers. This confinement takes especially place when liquids are involved since these produce large and unwanted capacitive

coupling between input and output electrical transducers. This coupling dramatically deteriorates the transfer function and is an important issue for the instrumentation of the sensors.

The sensor is a delay line formed by the transducers and the distance separating them. Each transducer is identified to its midpoint. The distance between the midpoints is L . The sensing part is located between the transducers and covers a total length D so that $D \leq L$. The guided mode propagates with a phase velocity $V = \omega/k$, where $\omega = 2\pi f$ is the angular frequency and $k = 2\pi/\lambda$ is the wavenumber. The waveguide is dispersive when the group velocity $V_g = d\omega/dk$ differs from the phase velocity.

The velocity is a function of the frequency and of the surface density $\sigma = M/A$ for a mass M per surface area A . This surface density can be defined as well in terms of material density ρ and thickness d by $\sigma = \rho d$. The phase velocity for an initial and constant mass σ_0 is denoted V_0 , and the group velocity V_{g0} . In the sensing part, the phase velocity is V and the group velocity V_g . According to this model, the transit time τ of this delay line is given by:

$$\tau = \frac{D}{V} + \frac{L - D}{V_0}. \quad (1)$$

Electromagnetic interferences are due to the cross-talk between the IDTs. The electromagnetic wave (EM) emitted by the input transducer travels much faster than the acoustic wave and therefore is detected at the output transducer without noticeable delay. At the output transducer, the two kinds of waves interact with an amplitude ratio, denoted by α , that creates interference patterns in the transfer function $H(\omega)$ of the delay line. The transfer function itself is given by the ratio of the output to the input voltages. The

transfer function with electromagnetic interferences is modelled by the following equation:

$$H(\omega) = \underbrace{H_0(\omega) \exp(-i\omega\tau)}_{\text{delay line}} + \underbrace{\alpha H_0(\omega)}_{\text{EM coupling}}. \quad (2)$$

The transfer function $H_0(\omega)$ is associated to the design of the transducers. The total transfer function can be rewritten as $H(\omega) = \|H(\omega)\| \exp(i\phi)$ where expressions for the amplitude $\|H(\omega)\|$ and the phase ϕ are obtained with help of complex algebra:

$$\|H(\omega)\| = \|H_0(\omega)\| \left\| \sqrt{1 + 2\alpha \cos(\omega\tau) + \alpha^2} \right\|; \quad (3)$$

$$\phi = \phi_0 - \arctan\left(\frac{\sin(\omega\tau)}{\alpha + \cos(\omega\tau)}\right). \quad (4)$$

The phase ϕ_0 corresponds to the packaging of the sensor and is due to different aspects linked to the instrumentation. It will be assumed independent of the frequency and of the sensing event. The relations (3) and (4) are the sources of ripples in the transfer function at the ripple frequency $\Delta\omega = 2\pi/\tau$. The relative amplitude peak to peak of the perturbation on the amplitude has a maximum effect (in dB) equals to $40 \log[(1 + \alpha)/(1 - \alpha)]$. The amplitude (in dB and normalized to have $\|H_0(\omega)\| = 1$) and the phase (in radians) as a function of the frequency are simulated in Figures 1 to 4 for different values of α .

Under the influence of the interferences, the phase has different behaviors function of α :

- (1) when $\alpha = 0$ (no interferences), the phase is linear with the frequency and has a periodicity equal to 2π (Fig.1);
- (2) when $\alpha < 1$, the phase is deformed but has still a periodicity equal to 2π

(Fig. 2);

(3) when $\alpha = 1$, the phase has a periodicity equal to π (Fig. 3);

(4) when $\alpha > 1$, the periodicity is lower than π (Fig. 4);

(5) when $\alpha \rightarrow \infty$, the phase is not periodic anymore and its value tends to ϕ_0 .

This specific behavior of the phase has to be considered for the evaluation of the gravimetric sensitivity.

3 Gravimetric sensitivity

Changes in the boundary condition of the waveguide due to the sensing event modify phase and group velocities. As consequence, the transit time of the delay line and the phase of the transfer function are modified. The sensing event is quantified by recording the phase shift at a fixed frequency (open loop configuration) or the frequency shift at a fixed phase (closed loop configuration). This quantification gives rise to the concept of sensitivity. The sensitivity is the most important parameter in design, calibration and applications of acoustic waveguide sensors. Its measurement must be carefully addressed in order to extract the intrinsic properties of the sensor.

3.1 Sensitivity definitions

The *gravimetric sensitivity* S_V is defined by the change of phase velocity as a function of the surface density change at a constant frequency. Its mathemat-

ical expression is given by Ref. (14):

$$S_V = \frac{1}{V} \frac{\partial V}{\partial \sigma} \Big|_{\omega}. \quad (5)$$

The definition reflects the velocity change in the sensing area only while outside this area the velocity remains unmodified. The expression is general because the initial velocity V of the sensing part does not need to be equal to V_0 ; this situation occurs in practical situations where the sensing part has a selective coating with its own mechanical properties, leading to a difference between V and V_0 .

In order to link the gravimetric sensitivity (caused by the unknown velocity shift) to the experimental values of phase and frequency shifts, we introduce two additional definitions related to the open and the close loop configurations, respectively. The *phase sensitivity* S_ϕ is defined by

$$S_\phi = \frac{1}{kD} \frac{d\phi}{d\sigma}, \quad (6)$$

and the *frequency sensitivity* S_ω is defined by

$$S_\omega = \frac{1}{\omega} \frac{d\omega}{d\sigma}. \quad (7)$$

3.2 Phase differentials without interferences

In order to point clearly the effects of the electromagnetic interferences on the different sensitivities presented in the previous section, we calculate the phase differentials in the ideal case of no interferences. For that case, the phase of the transfer function is a function of the frequency and the velocity, itself function of the frequency and the surface density:

$$\phi(\omega, V(\omega, \sigma)) = -\omega\tau \quad (8)$$

$$= -\omega \left(\frac{D}{V} + \frac{L-D}{V_0} \right). \quad (9)$$

Therefore, its total differential is:

$$d\phi = \left(\frac{\partial\phi}{\partial\omega} \Big|_{\sigma} + \frac{\partial\phi}{\partial V} \Big|_{\omega} \frac{\partial V}{\partial\omega} \Big|_{\sigma} \right) d\omega + \frac{\partial\phi}{\partial V} \Big|_{\omega} \frac{\partial V}{\partial\sigma} \Big|_{\omega} d\sigma. \quad (10)$$

The derivative of the phase velocity as a function of the frequency comes from the definitions of phase and group velocities; at constant surface density we have from Ref. (12):

$$\frac{\partial V}{\partial\omega} \Big|_{\sigma} = k^{-1} \left(1 - \frac{V}{V_g} \right). \quad (11)$$

The other partial differentials are obtained by differentiation of Equation (8):

$$\frac{\partial\phi}{\partial V} \Big|_{\omega} = \frac{\omega D}{V^2}; \quad (12)$$

$$\frac{\partial\phi}{\partial\omega} \Big|_{\sigma} = - \left(\frac{D}{V_g} + \frac{L-D}{V_{g0}} \right). \quad (13)$$

Furthermore, we also compute Equation (10) for a constant mass, that is for $d\sigma = 0$:

$$\frac{d\phi}{d\omega} = D \left(\frac{1}{V} - \frac{2}{V_g} \right) - \frac{(L-D)}{V_{g0}}. \quad (14)$$

This latter expression corresponds to $-\tau$ and is in agreement with the case without dispersion that gives the same transit time as modelled by Equation (1):

$$\frac{d\phi}{d\omega} = - \left(\frac{D}{V} + \frac{L-D}{V_0} \right) = -\tau \quad (15)$$

3.3 Open loop configuration

In the open loop configuration, the input transducer is excited at a given frequency while the phase difference between output and input transducers is recorded. This configuration with a constant frequency has $d\omega = 0$ in Equation (10); related phase variations caused by surface density variations are obtained by

$$\frac{d\phi}{d\sigma} = \left. \frac{\partial\phi}{\partial V} \right|_{\omega} \left. \frac{\partial V}{\partial\sigma} \right|_{\omega} \quad (16)$$

$$= \left. \frac{\partial\phi}{\partial V} \right|_{\omega} V S_V. \quad (17)$$

In the absence of interferences, phase variations obtained experimentally are directly linked to velocity changes by the product kD involving the geometry of the sensor as seen by replacing Equation (12) in Equation (17):

$$\frac{d\phi}{d\sigma} = kD S_V. \quad (18)$$

In other words: $S_\phi = S_V$ when there are no interferences. In a first approximation k is assumed equal to k_0 determined by the periodicity of the interdigitated electrodes in the transducer. This assumption is valid as long as the phase shift is evaluated close to the central frequency $\omega_0 = V_0 k_0$ and for waveguides with low dispersion. The wavelength is only known when the sensing part extends to the transducers ($D = L$). In that case, the transfer function of the transducers is modified as well by the velocity changes. In practice the value of the sensitivity is slightly underestimated to its exact value since $k \leq k_0$, the error being of the order of 5%.

In the case where interferences occur, the partial differential of ϕ with respect

to the velocity is obtained by differentiation of Equation (4):

$$\left. \frac{\partial \phi}{\partial V} \right|_{\omega} = \left(\frac{1 + \alpha \cos(\omega\tau)}{1 + 2\alpha \cos(\omega\tau) + \alpha^2} \right) \frac{\omega D}{V^2}, \quad (19)$$

and the phase sensitivity is obtained by combining the latter equation with Equation (17):

$$S_{\phi} = \left(\frac{1 + \alpha \cos(\omega\tau)}{1 + 2\alpha \cos(\omega\tau) + \alpha^2} \right) S_V. \quad (20)$$

The influence of electromagnetic interferences on the phase sensitivity is simulated in Figure 5 versus the relative frequency for different examples of α . The phase sensitivity is always different compared to the gravimetric sensitivity. For the threshold value $\alpha = 1$, the phase sensitivity is half of the gravimetric sensitivity; for higher values of α , the phase sensitivity is always underestimated to the gravimetric sensitivity.

3.4 Closed loop configuration

In the closed loop configuration, the frequency is recorded while a feedback loop keeps the phase difference between output and input transducers constant. To obtain the equivalent type of expression as in the open loop configuration, the total differential of the phase given by Equation (10) is rewritten in terms of frequency and surface density:

$$d\phi = \left. \frac{\partial \phi}{\partial \omega} \right|_{\sigma} d\omega + \left. \frac{\partial \phi}{\partial \sigma} \right|_{\omega} d\sigma. \quad (21)$$

The configuration at constant phase has $d\phi = 0$, the variation of the frequency as a function of the mass change is given by introducing this condition in

Equation (21):

$$\frac{d\omega}{d\sigma} = - \left(\frac{\partial\phi}{\partial\sigma} \Big|_{\omega} \right) / \left(\frac{\partial\phi}{\partial\omega} \Big|_{\sigma} \right). \quad (22)$$

The upper term is replaced by Equation (17). The phase slope as a function of the frequency at constant mass is obtained by differentiation of Equation (4):

$$\frac{\partial\phi}{\partial\omega} \Big|_{\sigma} = \frac{-\tau - \alpha(\tau - \omega\tau') \cos(\omega\tau) + \alpha^2\omega\tau'}{1 + 2\alpha \cos(\omega\tau) + \alpha^2} \quad (23)$$

where τ is exactly given by Equation (14). The derivative of the transit time τ' is calculated as

$$\tau' = \frac{\partial\tau}{\partial\omega} \Big|_{\sigma} \quad (24)$$

$$= - \left(\frac{D(V_g - V)}{\omega V V_g} + \frac{(L - D)(V_{g0} - V_0)}{\omega V_0 V_{g0}} \right). \quad (25)$$

When the waveguide is not dispersive, $\tau' = 0$ and Equation (23) is simpler.

We can establish a finalized equation taking into account the electromagnetic interferences by combining Equations (19) and (23) in Equation (22):

$$S_{\omega} = \left(\frac{1 + \alpha \cos(\omega\tau)}{\tau + \alpha(\tau - \omega\tau') \cos(\omega\tau) - \alpha^2\omega\tau'} \right) \frac{DS_V}{V}. \quad (26)$$

In the absence of interferences, if the waveguide has no dispersion and $V = V_0$, frequency variations obtained experimentally are directly linked to the gravimetric sensitivity by the ratio D/L as seen by replacing the transit time obtained via Equation (15) in Equation (26):

$$S_{\omega} = \frac{D}{L} S_V. \quad (27)$$

When the waveguide is dispersive, the transit time τ contains the combined information of the group velocities in the transducing and sensing part and the phase velocity in the sensing part. If the sensing part extends to the entire delay line ($D = L$) and still in the absence of interferences, we obtain:

$$S_\omega = \frac{V_g}{2V - V_g} S_V \quad (28)$$

that differs slightly from the result obtained previously by Jakoby *et al.* (14) who proposed the relation

$$S_\omega = \frac{V_g}{V} S_V. \quad (29)$$

In the case where interferences occur, the sensitivity is modified according to the value of α and is strongly dependent of the structure of the sensor and the velocities in the different parts of the sensor. A simple expression can not be deduced easily and the link between the frequency sensitivity and the gravimetric sensitivity is difficult to exploit.

4 Experimental results

For the practical consideration of the described behavior, we investigated a Love mode sensor. It was fabricated and tested under liquid conditions to evaluate the influence of the electromagnetic interferences. The Love mode was obtained by conversion of a surface skimming bulk wave (SSBW) launched in the direction perpendicular to the crystalline X axis of a 500 μm thick ST-cut (42.5° Y-cut) quartz substrate. The conversion was achieved by a 1.2 μm thick overlayer of silicon dioxide deposited on the top side of the substrate

by plasma enhanced chemical vapor deposition (Plasmalab 100 from Oxford Plasma Technology, England). Vias were etched in the silicon dioxide layer using a standard SF₆/O₂ plasma etch recipe. This process stopped automatically on the aluminium contact pads of the transducers.

The transducers consist of split fingers electrodes etched in 200 nm thick sputtered aluminium. The fingers are 5 μm wide and equally spaced by 5 μm . This defines a periodicity λ_0 of 40 μm . The acoustic aperture defined by the overlap of the fingers is equal to $80\lambda_0$ (= 3.2 mm), the total length of each IDT is $100\lambda_0$ (= 4 mm) and the distance center to center of the IDTs is $225\lambda_0$ ($L= 9$ mm, $D= 5$ mm).

The sensing area was defined by covering the space left between the edges of the IDTs by successive evaporation and lift-off of 10 nm of titanium and 50 nm of gold in a first experiment, and 200 nm of gold in a second experiment. The fingers were protected against liquid by patterning photosensitive epoxy SU-8 2075 (Microchem Corp., MA) defining 200 μm thick and 80 μm wide walls around the IDTs. Quartz glasses of 5 by 5 mm² were glued on top of the walls to finalize the protection of the IDTs.

The device was mounted and wire-bonded to an epoxy printed circuit board and its transfer function was recorded on a HP4396A Network Analyzer. This setup corresponds to the open loop configuration. Epoxy around the device covered and protected it and defined a leak-free liquid cell. The sensing area was immersed in a solution of KI/I₂ (4 g and 1 g respectively in 160 ml of water) that etched the gold away of the surface (17). The transfer function of the device was recorded every 4 seconds (limited by the GPIB transfer speed) during the etching of the gold with a resolution of 801 points over a span

of 2 MHz centered around 123.5 MHz. The initial transfer function of the device is presented in Figure 6 with and without gold. The transfer function during etching of the 200 nm is shown at two moments (44 seconds and 356 seconds after etching start) in Figure 7. The total time for this etching was approximately 620 seconds. The sensitivity was calculated by etching of 50 nm of gold and assuming a density $\rho = 19.6 \text{ g/cm}^3$. The result is plotted versus the frequency in Figure 8.

5 Discussion

Electromagnetic interferences have a clear effect on the transfer function because of the ripples they cause. The interaction modelled as a constant factor α is specific to each device and must be identified via a careful inspection of the transfer function. The amplitude of the transfer function peak to peak is supposed to be the product between the transfer function of the transducers and the interference, and therefore an evaluation of α is possible if the transfer function of the transducers only is known. However, the experiment shows that α is a function of the frequency and the surface density, indicating that finding its exact value is not straightforward. Only the phase indicates whether α is higher or lower than one.

In term of sensitivity, when $\alpha \geq 1$ the phase has a periodicity P in the range 0 to π . We suggest the following correction to the experimental phase sensitivity:

$$S_\phi = \frac{2\pi}{P} \frac{1}{kD} \frac{d\phi}{d\sigma}. \quad (30)$$

This modification gives a better evaluation of the gravimetric sensitivity by

stretching the phase of the transfer function to 2π . Only the extraction of P is not immediate since it depends upon α .

Finally, we must mention that the experimental part is not exactly providing a differential surface density $d\sigma$. Indeed, etching of 50 nm of gold corresponds to a surface density change of $98 \mu\text{g}/\text{cm}^2$. This is a relatively large shift compared to the targeted biochemical recognition application where protein films surface density are in the order of $500 \text{ ng}/\text{cm}^2$. The evaluation of the sensitivity is best recorded by adding or etching thin layers of materials and that under the operating conditions of the sensor, especially if liquids are involved (18).

6 Conclusion

We have proposed a model for surface acoustic waveguides used as sensors. The model shows the influence of electromagnetic interferences caused by interdigital transducers on the gravimetric sensitivity in open and closed loop configurations. In both cases, the dimensions of the delay line and the sensing part influence the experimental value of phase or frequency shifts.

In an open loop configuration and with interferences, the *phase* shift is disturbed and the sensitivity is over- or under-estimated to the value of the gravimetric sensitivity. For strong interferences, the phase has a periodicity lower than 2π that must be considered when normalizing the phase shift to obtain a correct figure of the sensitivity.

In a closed loop configuration and with interferences, the *frequency* shift is disturbed. The frequency shift is proportional to the sensitivity by the ratio between the length of the sensing area and the distance separating the

transducers. In addition, the frequency shift is influenced by the dispersive properties of the waveguide.

The influence of the electromagnetic interferences on the transfer function of a Love mode sensor operating in liquid conditions was presented for a comparison. From the experiment it appears that the interferences are function of both the frequency and the surface density.

For future investigations, an analytical expression of the electromagnetic-acoustic interaction and the parameters acting on it have to be identified in order to reduce the influence or, on the opposite, to enhance the gravimetric sensitivity of surface acoustic waveguides.

7 Acknowledgements

L. Francis is thankful to N. Posthuma for the support with the PECVD tool, to C. Bartic for the SU8 walls fabrication, and to the belgian F.R.I.A. fund for financial support.

References

- [1] C. Campbell, *Surface acoustic wave devices and their signal processing applications*, Academic Press, San Diego (1989).
- [2] B. A. Auld, *Acoustic Fields and Waves in Solids*, vol. 2., Wiley, New-York (1973).
- [3] K. Kalantar-Zadeh, W. Wlodarski, Y. Y. Chen, B. N. Fry, and K. Galat-

- sis, Novel Love mode surface acoustic wave based immunosensors, *Sensors and Actuators B* **91** (2003) 143–147.
- [4] O. Tamarin, C. Déjous, D. Rebière, J. Pistré, S. Comeau, D. Moynet, and J. Beziau, Study of acoustic Love wave device for real time bacteriophage detection, *Sensors and Actuators B* **91** (2003) 275–284.
- [5] E. Gizeli, Design considerations for the acoustic waveguide biosensor, *Smart. Mater. Struct.* **6** (1997) 700–706.
- [6] G. L. Harding, J. Du, P.R. Dencher, D. Barnett, and E. Howe, Love wave acoustic immunosensor operating in liquid, *Sensors and Actuators A* **61** (1997) 279–286.
- [7] F. Herrmann, M. Weinacht, and S. Büttgenbach, Properties of sensors based on shear-horizontal surface acoustic waves in $\text{LiTaO}_3/\text{SiO}_2$ and Quartz/ SiO_2 structures, *IEEE Trans. Ultrasonics, Ferroelectrics Freq. Control*, UFFC **48** (2001) 268–273.
- [8] S.-Y. Chu, W. Water, and J.-T. Liaw, An investigation of the dependence of ZnO film on the sensitivity of Love mode sensor in ZnO/Quartz structure, *Ultrasonics* **41** (2003) 133–139.
- [9] A. Rasmusson and E. Gizeli, Comparison of poly(methylmethacrylate) and Novolak waveguide coatings for an acoustic biosensor, *J. App. Phys.* **90** (2001) 5911–5914.
- [10] G. L. Harding, Mass sensitivity of Love-mode acoustic sensors incorporating silicon dioxide and silicon-oxy-fluoride guiding layers, *Sensors and Actuators A* **88** (2001) 20–28.
- [11] J. Du and G. L. Harding, A multilayer structure for Love-mode acoustic sensors, *Sensors and Actuators A* **65** (1998) 152–159.
- [12] G. McHale, F. Martin, and M. I. Newton, Mass sensitivity of acoustic wave devices for group and phase velocity measurements, *J. App. Phys.*

92(6) (2002) 3368–3373.

- [13] B. Jakoby and M. J. Vellekoop, Analysis and optimization of Love wave liquid sensors, *IEEE Trans. Ultrasonics, Ferroelectrics Freq. Control, UFFC* **45** (1998) 1293–1302.
- [14] B. Jakoby and M. Vellekoop, Properties of Love waves: applications in sensors, *Smart. Mater. Struct.* **6** (1997) 668–679.
- [15] Z. Wang, J. D. N. Cheeke, and C. K. Jen, Sensitivity analysis for Love mode acoustic gravimetric sensors, *App. Phys. Lett.* **64** (1994) 2940–2942.
- [16] R. M. White and F. W. Voltmer, Direct piezoelectric coupling to surface elastic waves, *App. Phys. Lett.* **7** (1965) 314–316.
- [17] J. L. Vossen and W. Kern, *Thin film processes*, Academic Press, New-York (1978).
- [18] J.-M. Friedt, L. Francis, K.-H. Choi, F. Frederix, and A. Campitelli, Combined atomic force microscope and acoustic wave devices: Application to electrodeposition, *J. Vac. Sci. Technol. A* , **21**(4), Jul/Aug 2003.

Fig. 1. Relative insertion loss (top) and phase (bottom) of the transfer function for $\alpha = 0$.

Fig. 2. Relative insertion loss (top) and phase (bottom) of the transfer function for $\alpha = 1/2$.

Fig. 3. Relative insertion loss (top) and phase (bottom) of the transfer function for $\alpha = 1$.

Fig. 4. Relative insertion loss (top) and phase (bottom) of the transfer function for $\alpha = 2$.

Fig. 5. Phase sensitivity at constant frequency as a function of the relative frequency for different values of simulated interferences obtained by Equation (20).

Fig. 6. Initial aspect of the experimentally recorded transfer function of the Love mode sensor with (dashed line) and without (solid line) an overlayer of 200 nm of gold. This device presents an initial phase $\phi_0 = \pi$, leading to a vertical offset by π compared to the simulated phase curve represented in Fig. 2.

Fig. 7. Aspect of the experimentally recorded transfer function at two different moments of the etching of 200 nm of gold (solid line after 44 seconds and dashed line after 356 seconds). The solid line shows a value of α close to 1 around 123.5 MHz.

Fig. 8. Phase sensitivity computed with help of the experimental data obtained from etching of 50 nm of gold as a function of the frequency. Oscillations are attributed to electromagnetic interferences.

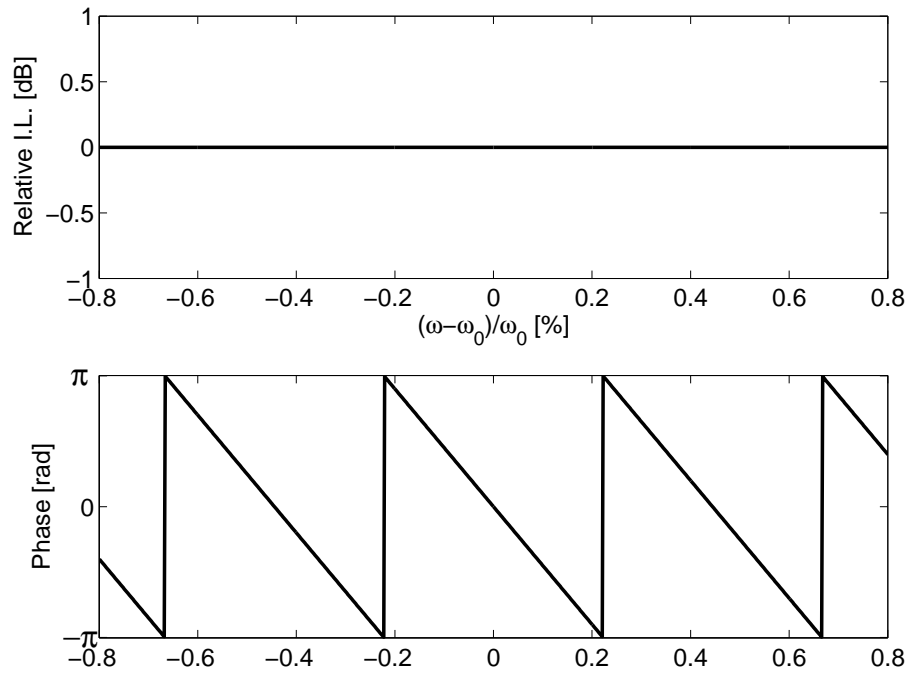


Figure 1

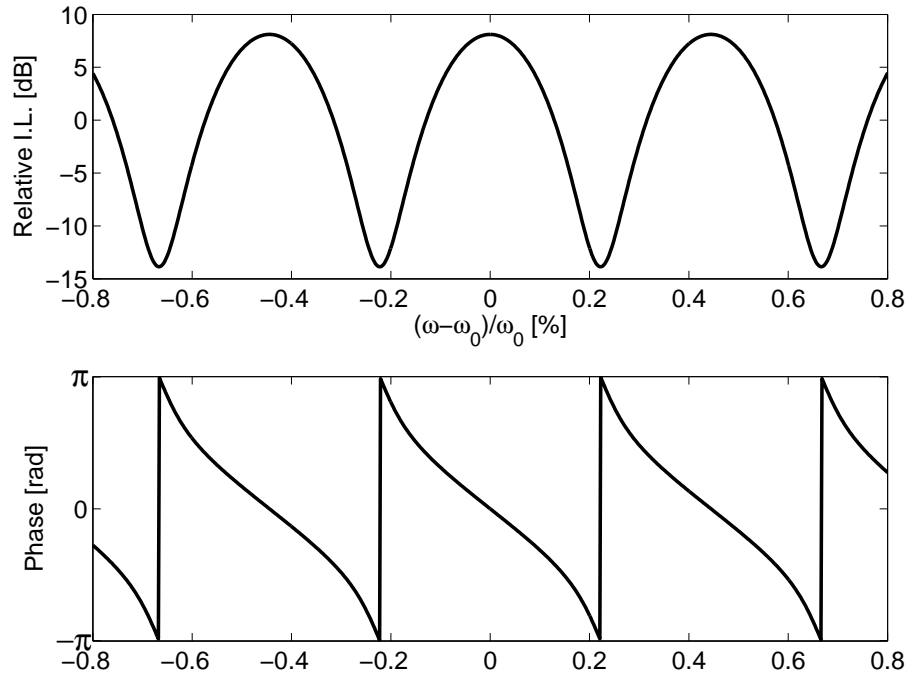


Figure 2

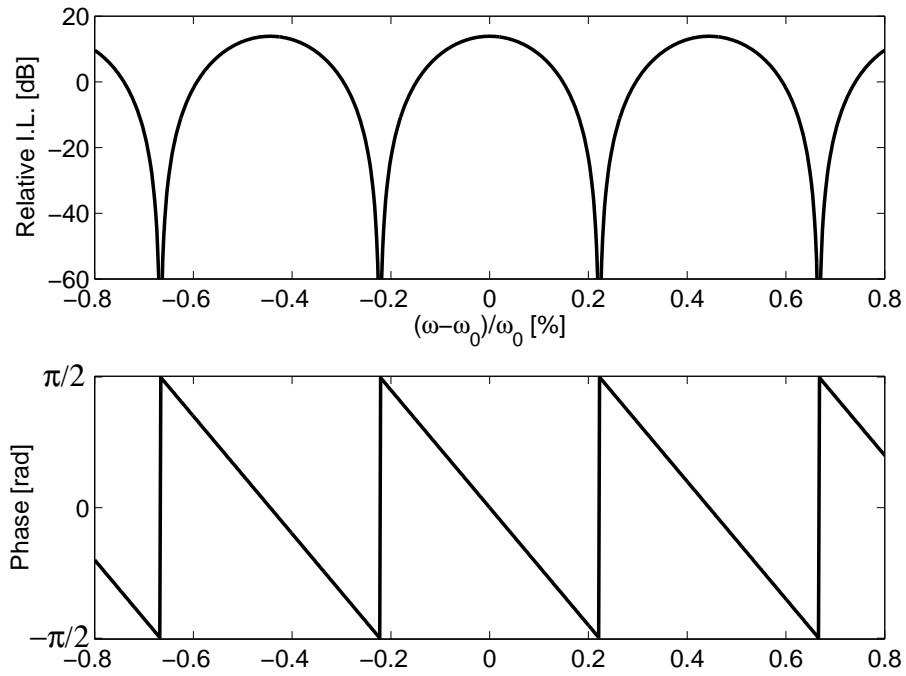


Figure 3

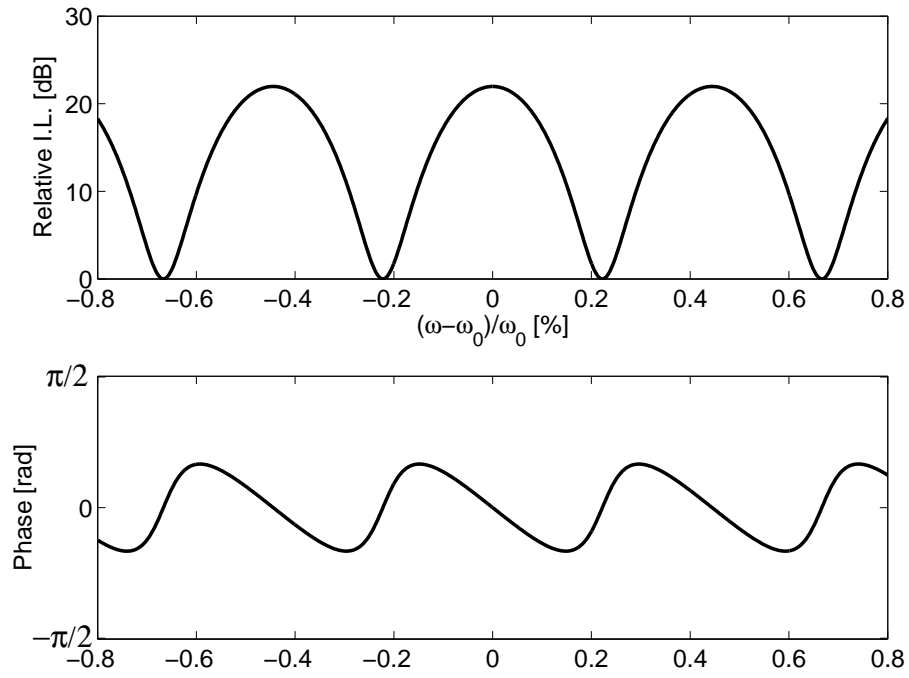


Figure 4

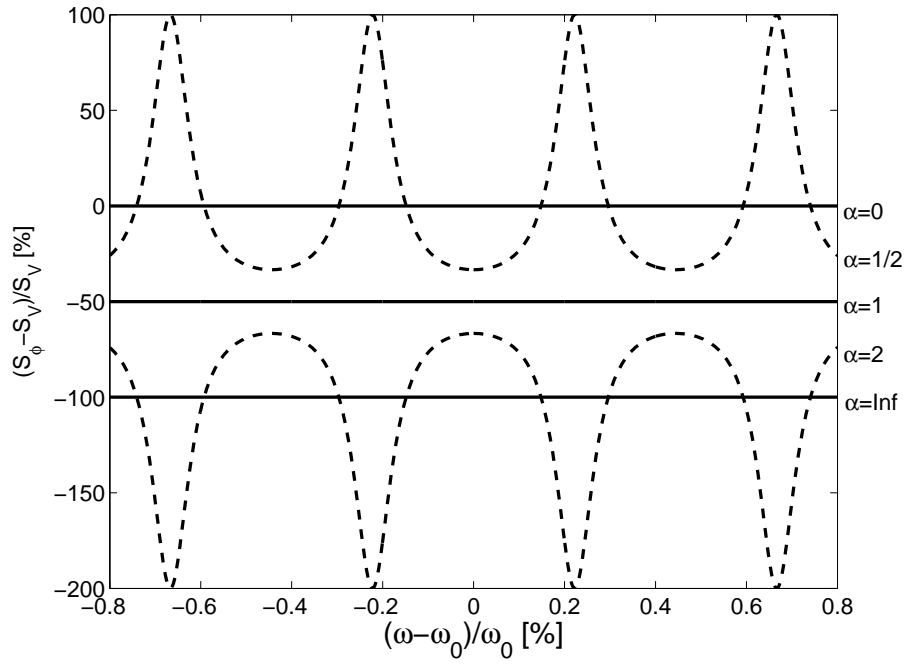


Figure 5

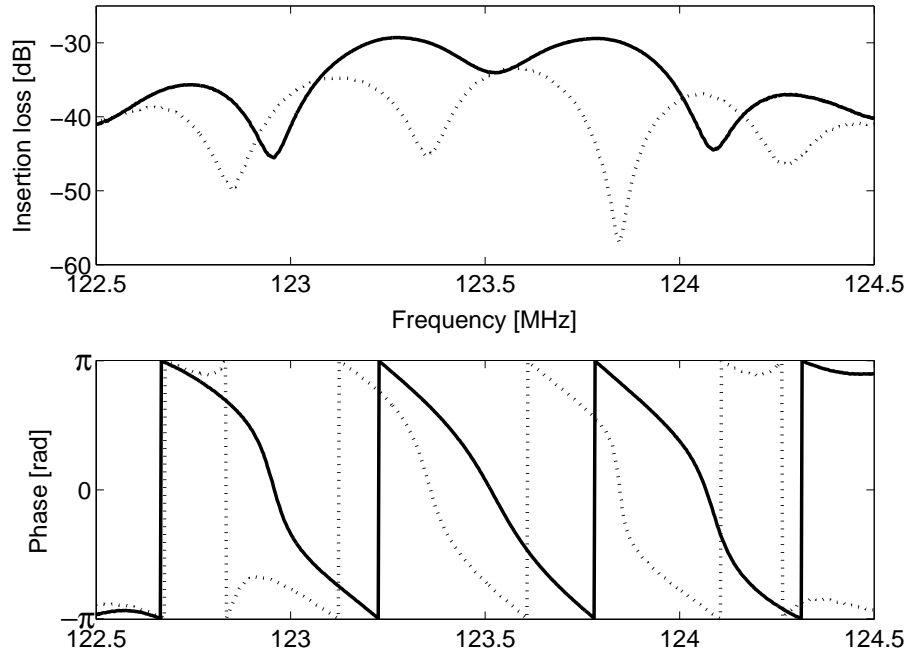


Figure 6

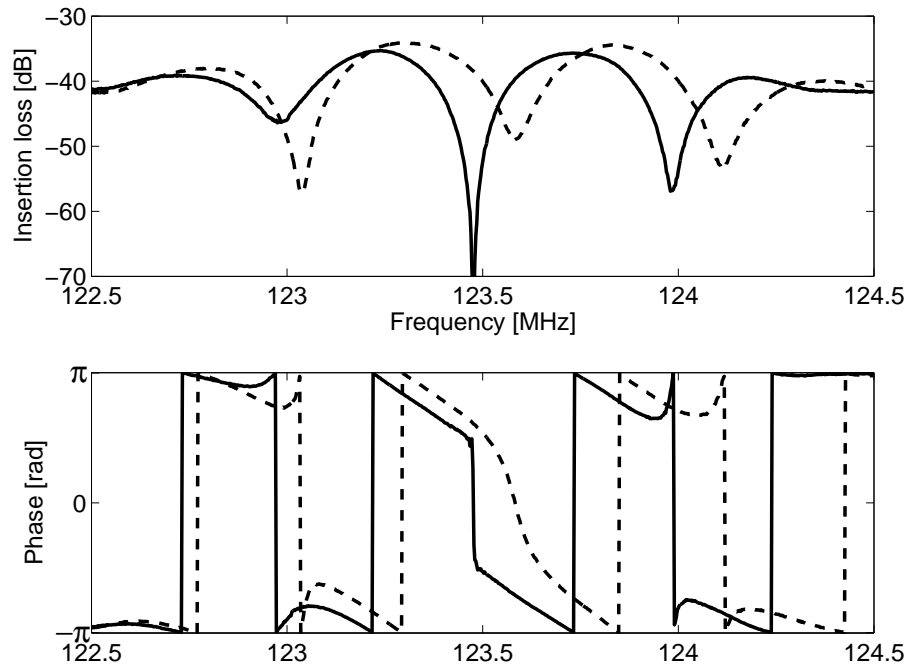


Figure 7

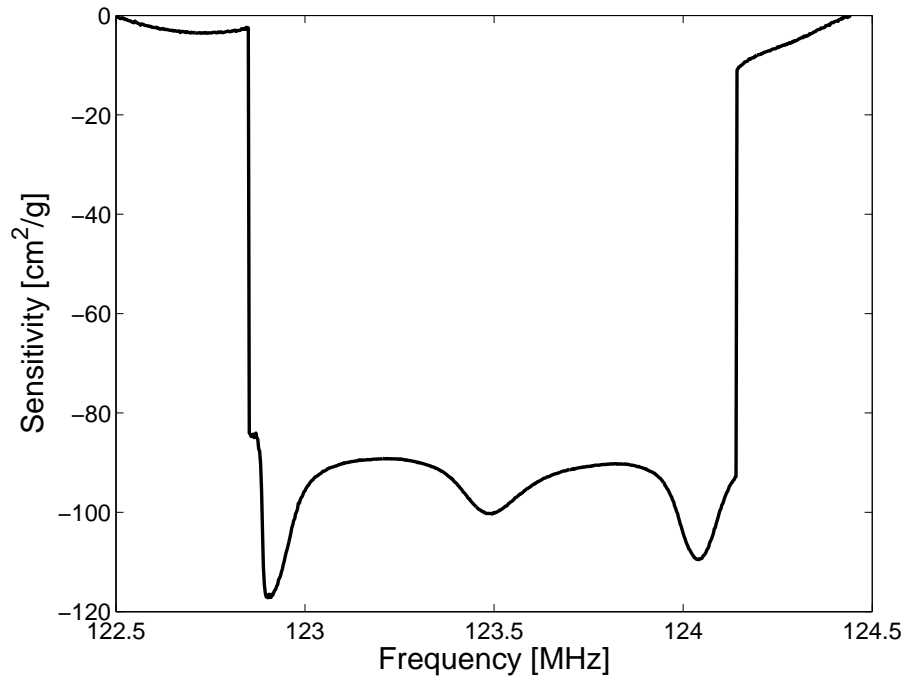


Figure 8